Coordination sphere of the third metal site is essential to the activity and metal selectivity of alkaline phosphatases

Dimitris Koutsioulis,[1,2] Andrzej Lyskowski,[3] Seija Mäki,[3] Ellen Guthrie,[1] Georges Feller,[4] Vassilis Bouriotis,[2] and Pirkko Heikinheimo[3]*

[1]New England Biolabs Inc., 240 County Road, Ipswich, Massachusetts 01938-2723

[2]Department of Biology, University of Crete, Heraklion, Crete, Greece

[3]Structural Biology and Biophysics, Institute of Biotechnology, University of Helsinki, Helsinki, FIN-00014 Finland

[4]Laboratory of Biochemistry, Centre for Protein Engineering, University of Liège, Institute of Chemistry B6a, Liège-Sart Tilman, Belgium

Received 6 July 2009; Revised 7 September 2009; Accepted 23 October 2009
DOI: 10.1002/pro.284
Published online 13 November 2009 proteinscience.org

Abstract: Alkaline phosphatases (APs) are commercially applied enzymes that catalyze the hydrolysis of phosphate monoesters by a reaction involving three active site metal ions. We have previously identified H135 as the key residue for controlling activity of the psychrophilic TAB5 AP (TAP). In this article, we describe three X-ray crystallographic structures on TAP variants H135E and H135D in complex with a variety of metal ions. The structural analysis is supported by thermodynamic and kinetic data. The AP catalysis essentially requires octahedral coordination in the M3 site, but stability is adjusted with the conformational freedom of the metal ion. Comparison with the mesophilic *Escherichia coli*, AP shows differences in the charge transfer network in providing the chemically optimal metal combination for catalysis. Our results provide explanation why the TAB5 and *E. coli* APs respond in an opposite way to mutagenesis in their active sites. They provide a lesson on chemical fine tuning and the importance of the second coordination sphere in defining metal specificity in enzymes. Understanding the framework of AP catalysis is essential in the efforts to design even more powerful tools for modern biotechnology.

Keywords: crystal structure; enzyme mechanism; extremophile; metal catalysis; psychrophile

Introduction

Alkaline phosphatases (AP; EC 3.1.3.1) are homodimeric enzymes that exist in various organisms from bacteria to mammals. Irrespective of their origin, APs catalyze the hydrolysis or transphosphorylation of a variety of phosphate monoesters.[1] AP has become a useful tool in molecular biology laboratories, because it is used as a marker for enzyme immunoassays and to remove 5′-terminal phosphates from DNA fragments.

The catalyzed reaction includes two steps, with the first one generating a covalent phosphoserine intermediate. In the second step, this intermediate is attacked by a nucleophilic water or alcohol to release inorganic phosphate or to generate a new phosphoester.[2] Although the natural pH-environment for APs is around neutral, their catalytic optima are more than pH 8.[3,4] At optimal pH, dephosphorylation of the covalent enzyme intermediate is fast, with the rate limiting step being the release of the noncovalent product phosphate. In acidic conditions

Additional Supporting Information may be found in the online version of this article.

Abbreviations: AP, alkaline phosphatase; ECAP, *Escherichia coli* alkaline phosphatase; TAP, alkaline phosphatase from TAB5.

Some of this work was supported by New England Biolabs, Inc., a company that may profit from the sale of enzymes described herein. The authors are (EPG) or were (DK) employees of New England Biolabs, Inc.

**Correspondence to:* Pirkko Heikinheimo, Structural Biology and Biophysics, Institute of Biotechnology, PO Box 65, University of Helsinki, Helsinki, FIN-00014 Finland. E-mail: pirkko.heikinheimo@helsinki.fi

(pH < 6), dephosphorylation of the covalent enzyme intermediate becomes rate-limiting.[3]

X-ray crystallography has been widely used to understand the stability and general architecture of the APs. Structures of *Escherichia coli* AP (ECAP),[1,2] human placental AP,[5,6] shrimp AP,[7] *Vibrio*,[8] and Antarctic strain TAB5 AP (TAP)[9] have been determined. The catalysis involves three metal ions, which bind to the M1–M3 sites in the active site. The hydroxyl group on the active site serine is first activated by the metal ion at the M2 site.[2] In the second step, a water molecule, activated by the M1 metal, hydrolyses the covalent intermediate to yield a free serine residue and a phosphate.[2] An arginine residue (R148 in TAP) coordinates the phosphoryl group,[2] and a positively charged area on the opposite side possibly assists in product release[9] by providing additional binding sites and thus directing the released phosphate molecule away from its primary binding site, similarly to the product release channel in inorganic phosphatases.[10] The binding sites for M1 and M2 are well conserved (Supporting Information Table I).

Unlike the tetrahedrally coordinated M1 and M2 binding sites, the M3 site is octahedral, and it is less conserved than the M1 and M2 sites (Supporting Information Table I). The functional role and specificity of the M3 metal are also poorly understood. It has been proposed that a water coordinated to M3 would act as a general acid and reprotonate the catalytic serine.[2,11] Alternatively, an M3 coordinated water could assist in leaving group activation by directly protonating the phosphate group.[2,12] The most common combination of catalytic metal ions for all of the sites is a mixture of Zn^{2+} and Mg^{2+} and occasionally Co^{2+} and Mg^{2+}.[13,14] The majority of the AP crystal structures have been determined with three Zn^{2+} ions at the active site, although Mg^{2+} at the M3 site is optimal for ECAP[2] and TAP catalysis (currently published).

Two residues have been proposed to affect ECAP metal specificity, residues D153 and K328 (H135 and W260 in TAP). Mutagenesis of the ECAP residue corresponding to TAP H135 (ECAP D153H) results in a tetrahedral M3 site, which is occupied by a Zn^{2+}.[15] The enzyme has decreased metal affinity, but at high concentrations of Mg^{2+} and combined with a mutation at D330, the enzyme is 17-fold more active than wild-type.[11,16]

TAP is a typical cold-adapted enzyme: it has naturally high catalytic activity but it is relatively unstable at high temperatures.[4] In a previous study, we modified TAP by laboratory evolution to identify the residues determining TAP activity and stability.[17] The mutation H135E increased the k_{cat} of TAP catalysis, although it also destabilized the enzyme.[17] To study the contribution of H135 in detail, we have also designed a single point mutation H135D,[18] which mimics the ECAP active site arrangement. This TAP variant has an increased activity and increased thermostability.[18]

In this study, we have determined three structures of the H135D- and H135E-TAP in complex with Mg^{2+} and Zn^{2+} or with Zn^{2+} only. The structures show that the basis for the metal selection at the M3 site is in the indirect, second coordination sphere of the metal ion and not in the direct, primary coordination of the metal. Both coordination spheres are differently organized in the psycrophilic TAP and mesophilic *E. coli* AP. The wtTAP, H135D-TAP, and H135E-TAP were also functionally and thermodynamically characterized in detail, supporting the results from the structural analysis.

Results

Structures reveal fine tuning of the active site metal content

We have determined the crystal structures of the two TAP variants, the H135D-TAP at 1.7 Å and 1.8 Å resolution, and H135E-TAP at 2.0 Å resolution. The mutations do not cause any significant changes in the overall structure of TAP; the Cα atoms of the A and B monomers of H135D superimpose on the wtTAP A and B monomers with an root mean square deviation (RMSD) of 0.18 and 0.22 Å, which is better than the overlay of the two H135D monomers, which superimpose with an RMSD of 0.42 Å. The main differences between the monomers are the outermost helical structures (formed by residues 172-193) on the side of the TAP dimer and the flexible "hat" loop region (located between residues 315–320), which was not built in the earlier structure of the wtTAP. The completed hat also allows us to better understand the dimer contacts: the dimers connect through space in a hand shaking manner, where the loop from monomer A makes a crystal contact with the same loop in monomer B in a symmetry related position (Supporting Information Fig. 2).

We first crystallized both variants in an analogous way as wtTAP,[9] without any preceding ethylenediaminetetraacetic acid (EDTA) treatment. The H135D-TAP showed an octahedrally coordinated metal in the M3 position which was too dense to be Mg^{2+}. The density could nicely fit a Zn^{2+} ion, which was unexpected considering the 1000-fold excess of Mg^{2+} in the crystallization and the Mg^{2+} bound to the wtTAP structure. Nonetheless, a change in the metal ions was somewhat expected, because the specific activity of H135D-TAP responds equally well to Zn^{2+} and Mg^{2+} after removal of the weakly bound metal ions (see later), whereas the wtTAP shows a strong preference for Mg^{2+}. However, because of the unexpected coordination number of the Zn^{2+} in M3, we wanted to verify the identity of the metal ion, and thus crystallized this variant after EDTA treatment with a mixture of Mg^{2+} and Zn^{2+} and with Zn^{2+} alone.

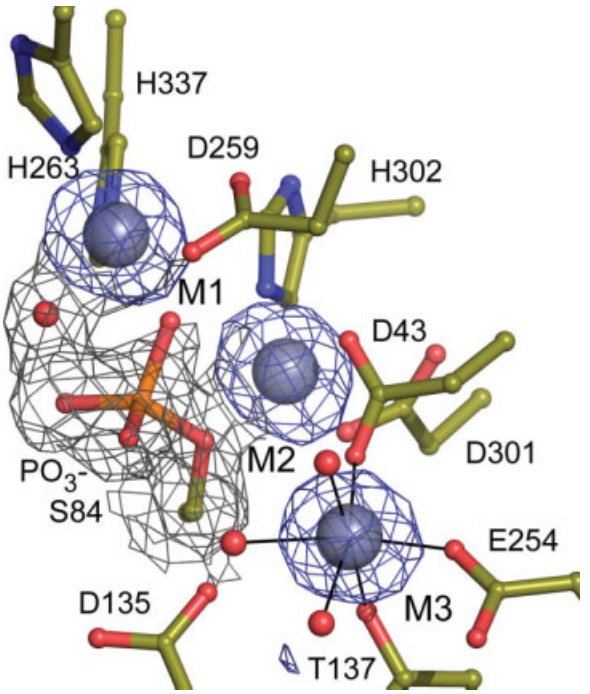

Figure 1. The 2FoFc map at 1.0 sigma on S84 and the anomalous difference map at 4.0 sigma on the three Zn^{2+} ions in the active site of the H135D-TAP structure. The difference map identifies all metal binding sites occupied with Zn^{2+}, although the M3 metal has an unexpected octahedral coordination sphere (coordination on M3 shown in black lines).

Anomalous diffraction from the structure of the H135D-TAP crystallized with only Zn^{2+} clearly identifies three Zn^{2+} ions in the active site, in positions M1 to M3 (Fig. 1). The M1 and M2 metal ions are tetrahedrally coordinated as in the wild-type, but M3 remains octahedrally coordinated, even though the identity of the metal is now Zn^{2+}. Coordination of six ligands is rare for Zn^{2+}, but in a few cases, it has been observed in catalytic Zn^{2+} binding sites.[19] In ECAP, the reverse mutation (D153H) also resulted in a change of metal ion in the M3 position, but in this structure Zn^{2+} is tetrahedrally coordinated.[20] Apparently, the Zn^{2+} affinity for the M3 site is quite strong, because in the same crystallization conditions, but without a preceding EDTA treatment, the H135D-TAP variant also crystallizes with Zn^{2+} at the M3 position (data not shown) even when it is crystallized in the presence of a 1000-fold excess of Mg^{2+}.

The H135E-TAP variant crystallizes like the wtTAP structure: with Zn^{2+} in M1 and M2 sites, but Mg^{2+} in M3. The identity of the metal ion can be clearly distinguished by the fit to the depth of the electron density. Mg^{2+} in the M3 site refined with B-factors of 10.04 and 14.26 $Å^2$ (Supporting Information Table II) with coordinating water B-factors from 15.72 to 29.93 $Å^2$, which are reasonable compared to the surrounding atoms. A Zn^{2+} atom at this density would yield much higher B-factors.

The active site of both variants is otherwise well conserved. M2 and M3 positions align perfectly to each other when the structures are superimposed, even if the nature of the metal ion at the M3 site has changed (Fig. 2). The hydration sphere of the metal ions is also well preserved. In all TAP variants, wtTAP (2iuc[9]), H135D-TAP, and H135E-TAP, M3 is coordinated by three water molecules and residues D43, T137, and E254 (Fig. 2). Thus, the site is preserved as octahedral, regardless of mutation or the identity of the metal at M3.

In the wtTAP structure,[9] we observed a large unassigned electron density in the vicinity of the M1 site and S84. We could not interpret the density with anything reasonable from the crystallization solution and decided to model the density with a phosphorus atom, showing only the central position for the attached phosphoryl group in the covalent intermediate during catalysis. We have observed similar density in all three variant structures, now with a slightly higher resolution. We tested whether the density could be phenylmethane sulphonylfluoride (PMSF), because the proteins had been treated with this compound during purification and PMSF is

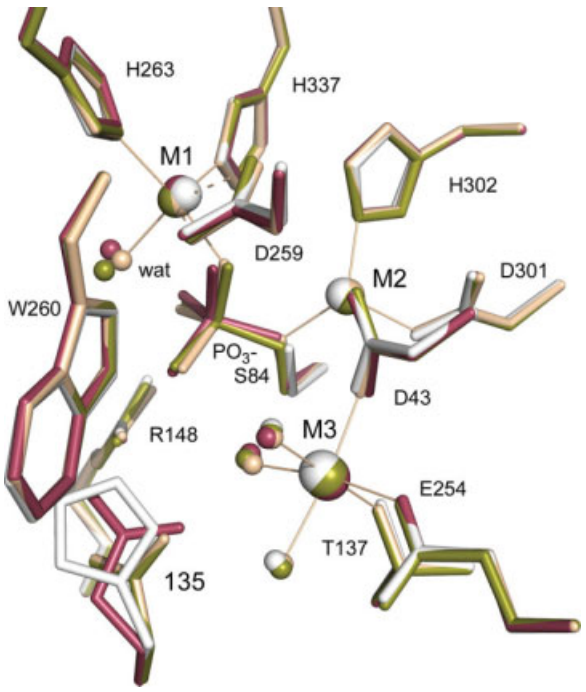

Figure 2. Overall structure of the active site. Positions of the side chains and metals are well preserved in all structures, regardless of the mutation. The structures also contain a covalently attached PO_3 group on S84 and a water molecule attached to M1 in a position suitable for hydrolyzing the PO_3-S84 bond. Structures are colored as follows: H135D-2$Zn^{2+}$$Mg^{2+}$-TAP in pale wheat, H135D-3Zn^{2+}-TAP in green, H135E-TAP in red, and the wtTAP[9] in white.

Table I. *Data and Structure Quality*

	H135D-3Zn	H135D-2ZnMg	H135E-2ZnMg
Wavelength (Å)	1.28224	1.28690	0.93300
Space group	$P2_12_12$	$P2_12_12$	$P2_12_12$
Unit cell (Å)			
a	70.11	70.32	70.42
b	173.32	173.02	173.19
c	55.19	54.97	55.44
Data			
Resolution[Å]	46.57-1.69	46.37-1.78	46.57-1.99
R_{pim}	0.050	0.055	0.055
Mean((I)/sd(I))	15.2	10.7	10.8
Completeness	99.6	98.9	99.8
Multiplicity	7.1	7.0	3.6
Refinement			
No. reflections (free)	118325 (1861)	108122 (3578)	80983 (1746)
R-factors before TLS refinement			
R_{work}/%	15.59	17.40	16.67
R_{free} /%	18.75	21.50	20.01
Final R-factors			
R_{work}/%	13.97	15.94	16.06
R_{free} /%	17.03	19.89	20.43
Final structure			
Total no.			
Atoms	6219	5839	5906
Waters	971	589	654
Metals	6	8	8
Deviation from ideal values			
Bonds/Å	0.008	0.006	0.006
Angles/°	1.147	1.021	1.003
Dihedrals/°	16.944	16.693	17.150
Ramachandran plot areas, residues in			
Preferred (%)	655 (95.0)	654 (95.0)	653 (94.9)
Allowed (%)	20 (2.9)	24 (3.5)	23 (3.3)
Outliers (%)	13 (1.9)	10 (1.5)	12 (1.7)

The free set of reflections was excluded from the refinement to monitor it. For definitions of the R-factors and R_{pim}, see Ref. 32.

known to covalently attach to proteases. However, PMSF does not inhibit TAP (data not shown), and the density does not support the phenyl end of the molecule, thus we decided to exclude this possibility. Because the electron density at higher resolution in the H135D-3Zn structure (Table I) now also has a very distinct shape, we have modeled the reaction intermediate S84-PO_3 and a water coordinated to M1 in all three structures (Fig. 2). The phosphate presumably originates from the PEG solution used during crystallization.[12] TAP is also crystallized at pH 6.5, where the release of the covalent intermediate is slow,[3] thus allowing traces of the product to be detected in the crystallized protein.

The wtTAP also has two external metal ions, bound outside of the active site. The variants that were crystallized with Mg^{2+} and Zn^{2+} also contain Mg^{2+} at site M5, but the M4 site did not seems to be occupied. This might be due to the different arrangement of unit cell axes in the current structures and wtTAP,[9] thus leaving M4 as a crystallographic artefact without true biological function. In the H135D-TAP structure, which was crystallized only in the presence of Zn^{2+}, the density at M5 is ambiguous and does not support a partially occupied metal ion nor does the anomalous difference map support a Zn^{2+} at M5. Thus the site is modeled with a water molecule.

Mutations on H135 change the catalytic efficiency of TAP

We measured k_{cat} and K_m for the generated TAP variants in standard reaction conditions for wtTAP: at pH 10 with 10 m*M* $MgCl_2$ and 1 m*M* $ZnCl_2$. Both TAP variants, H135E-TAP and H135D-TAP, are more active than the wtTAP and have 3- and 2-fold higher catalytic constants (k_{cat}) (Table II). However, substrate binding is less efficient, as the K_m value of both variants is greatly increased (Table II). As a

Table II. *Kinetic Parameters of wtTAP and Its H135 TAP Variants Using pNPP as Substrate With 10 mM $MgCl_2$ and 1 mM $ZnCl_2$ at 25°C*

Enzymes	K_m (m*M*)	k_{cat} (s^{-1})	k_{cat}/K_m ($s^{-1}\cdot mM^{-1}$)
WT	0.312	50.04	160.4
H135D	3.091	101.5	32.8
H135E	2.874	146	48.7

Table III. *The Effect of Metal Ions on Catalysis*

	Before dialysis [k_{cat} (s^{-1})] (1)	After dialysis [k_{cat} (s^{-1})] (2)	After dialysis with metals [k_{cat} (s^{-1})] (3)
wtTAP	50.04	0.46	30.44
H135D	101.5	15.6	105
H135E	146	1.28	117.6

Weakly bound metals were removed by extended dialysis in 20 m*M* Tris pH 7.6. AP activity toward the pNPP substrate was measured before treatment (1), after dialysis, and after loading the enzymes with 10 m*M* $MgCl_2$, and 1 m*M* $ZnCl_2$. k_{cat} values in (1) and (3) were determined in the same buffer as in Table II, whereas in (2), no metals were added. Reported values are the average of three measurements and standard deviations do not exceed 5%.

consequence, the catalytic efficiency k_{cat}/K_m is less favorable for the mutated enzymes.

Dialysis in metal free conditions decreases the k_{cat} of wtTAP and H135E-TAP more that 100-fold, underlining the importance of the metal ions on the activity of APs (Table III). Only the H135D-TAP variant remained significantly active after dialysis, retaining 15% of its initial k_{cat} (Table III). After the dialysis, we reintroduced metal ions to the samples separately and in combination $MgCl_2$, $ZnCl_2$, and $CoCl_2$. After Zn^{2+} and Mg^{2+} addition, H135D-TAP recovered full activity, whereas wtTAP and H135E-TAP regained 60 and 80% of their k_{cat} values (Table III), showing that although nearly inactive without the metal ions, the enzymes retain their overall fold during dialysis. However, the variants respond differently to the different metal ions (Table IV). H135D-TAP recovered almost full activity in the presence of both Mg^{2+} and Zn^{2+}, unlike wtTAP or H135E-TAP (Tables III and IV). With Zn^{2+} alone, the difference was even more remarkable, because H135D-TAP recovered 70% of its activity, whereas wt and H135E recovered only 4 and 17%, respectively. In all cases, addition of Co^{2+} alone had no significant effect on the specific activity of the enzymes, and in combination with Mg^{2+} it was less activating than Mg^{2+} alone or Mg^{2+} with Zn^{2+} (Table IV).

H135 contributes to the thermal stability of TAP

To test the M3 site effects on the thermal inactivation of TAP, we heat treated the purified wtTAP and H135D- and H135E-TAP variants at 55°C and 60°C for 120 min and subsequently measured the remaining (residual) activity in standard conditions. The wild-type enzyme is fairly sensitive to these temperatures, and 83% of the activity disappeared already after the first 5 min at 55°C (Table V). The mutation H135D had a strong stabilizing effect, and even after 2 hr at 55°C, H135D-TAP retained 42% of its activity, about 11 times that of wtTAP. Even after 2 hr at 60°C, 2.3% of the activity remained, whereas the wtTAP was almost completely inactivated (Table V). In contrast, H135E-TAP is sensitive to heat, and its activity is quickly destroyed in 60°C, approximately 14 times faster than the wtTAP (Table V). Thus, the identity of the residue at position 135 and the possible effect for metal coordination are important for the thermal stability of TAP.

Thermal unfolding of wtTAP has three transitions

The thermal unfolding of the wtTAP has a complex pattern in differential scanning calorimetry. Structural changes are evident already at 35°C (the heavy line in Fig. 3) and are followed by a main unfolding transition centered around 45°C. However, two additional unfolding transitions occur at higher temperatures (Fig. 3). Because the wtTAP unfolding is irreversible, and therefore kinetically driven, this also indicates that the unfolding pathway passes through at least three intermediate states differing in their kinetics of unfolding and resistance to heat denaturation. The unfolding curve of the least stable variant, H135E-TAP, is characterized by disappearance of intermediates at low and high temperatures and by a sharp transition around 50°C, indicating high unfolding cooperativity (Fig. 3). This is consistent with previously reported low kinetic stability in proteins displaying uniformly heat-labile structure that increases both the unfolding rate and cooperativity.[21] Interestingly, the H135D-TAP displays an intermediate behavior: it unfolds over a broad range of temperature, and thus has low unfolding cooperativity, but it has only one main transition around 56°C (Fig. 3). This mutant uniformly resists heat denaturation, and this could be correlated with its improved resistance to inactivation (Table V).

Table IV. *The Effect of Different Metal Ions on the Specific Activity of the Enzymes*

	Specific activity (%)						
	Before dialysis	No metals	Mg^{2+} Zn^{2+}	Mg^{2+} Co^{2+}	Mg^{2+}	Zn^{2+}	Co^{2+}
wtTAP	100	1.2	64	24	70	4.4	1.5
H135D	100	18	98	76	89	70	21
H135E	100	1	78	7	16	17	1

All values were determined at 25°C in a buffer containing 1 *M* diethanolamine-Cl pH 10, 10% glycerol and 5 m*M* pNPP in the presence or absence of 1 m*M* $MgCl_2$, 1 m*M* $ZnCl_2$, and 1 m*M* $CoCl_2$ (as indicated). Reported values are the average of at least three measurements, and standard deviations do not exceed 5%.

Table V. *Thermal inactivation of wtTAP and the H135 TAP variants at 55°C and 60°C*

	Activity (%)		
Heat treatment/min	wtTAP	H135D-TAP	H135E-TAP
At 55°C			
0	100	100	100
5	17.5	79.8	4
10	14.2	76	2.4
20	11.2	65.6	1.4
60	6.6	56.1	0.8
120	3.7	42	0.3
At 60°C			
0	100	100	100
5	9.9	30.5	0.7
10	6.3	17	0.5
20	3.2	9.7	0.4
60	1.3	4.4	0.2
120	0.6	2.3	0.09

Reported values are the average of at least three measurements, and standard deviations do not exceed 5%.

The unfolding pattern correlates with the calorimetric enthalpy of the mutants, which is calculated from the normalized area of the transition, and which corresponds to all enthalpy-driven interactions disrupted during unfolding. The normalized area of transition for the wtTAP shows ΔH_{cal} of 163 kcal/mol. The least stable variant H135E-TAP is drastically destabilized as judged from the low ΔH_{cal} value, 98 kcal/mol. Therefore, the enthalpic destabilization seems to be the primary determinant of the lower heat stability of its activity. Here again, the H135D-TAP displays an intermediate behavior: it is enthalpically destabilized (low ΔH_{cal}), but the unfolding transition occurs at a higher temperature (Fig. 3). Therefore, it seems that kinetic stabilization of H135D-TAP is the primary determinant of the improved heat stability of the activity.

Discussion

We have previously used random and rational mutagenesis to demonstrate that H135 in the vicinity of the M3 binding is important for wtTAP activity and stability.[14,15] In this study, we analyzed the structural and functional role of H135 in more detail in combination with metal ions. When the loosely bound metal ions are diluted away, both variants catalyze phosphate hydrolysis equally well with Mg^{2+} or Zn^{2+} when reconstituted, although the H135E variant prefers a mixture of the two metal ions (Table IV). This could indicate partial loss of also the metal ion at M1 and M2 positions, which are otherwise very tightly coordinated. The response to the metal addition is a clear difference from the wt enzyme, which catalyzes the reaction very poorly with reconstituted Zn^{2+} alone compared with Mg^{2+} alone or a mixture of the metal ions. The reason for this is evident from the crystal structures, which show a difference in metal selectivity at M3. The H135D variant in particular binds Zn^{2+} efficiently in the M3 position and does so in an activating manner through octahedral coordination of Zn^{2+}.

The catalytically fastest variant, H135E-TAP, is the least stable of the three studied proteins. It survives the dilution of metal ions to the same extent as wtTAP, but it has the highest k_{cat} after addition of the metal ions. Its activity is, however, quickly destroyed by heat. The H135E-TAP variant has sharp heat-induced unfolding transition with a low number of intermediates, as is typical for unstable proteins.[21] We believe that these changes are mostly due to changes at the M3 metal binding site. If M3 binding is weak, the metal ion is also more easily lost upon dialysis, resulting in lower stability. However, when metal ions are present in solution in adequate amounts, this weak binding also allows greater flexibility and faster catalysis by the H135E variant.

A combination of Mg^{2+} and Zn^{2+} provides the highest activity for both wild-type ECAP[2] and TAP (Table IV). Mg^{2+} is a common metal in enzyme-catalyzed hydrolysis of phosphoryl groups.[22] It provides suitable pK_a adjustments for catalytic waters[23] and suitable affinity and selectivity for the phosphate group, allowing fast product release from enzyme active sites. Coordination by oxygen is more typical for Mg^{2+} than for Zn^{2+}, which prefers cysteine and histidine residues for formation of its binding site.[24] Mg^{2+} also strictly prefers octahedral coordination, unlike Zn^{2+}, which can adopt both tetrahedral and octahedral coordination.[19] In the TAP active site, the M3 site is formed by D and E coordination and by a neutral threonine and three water molecules

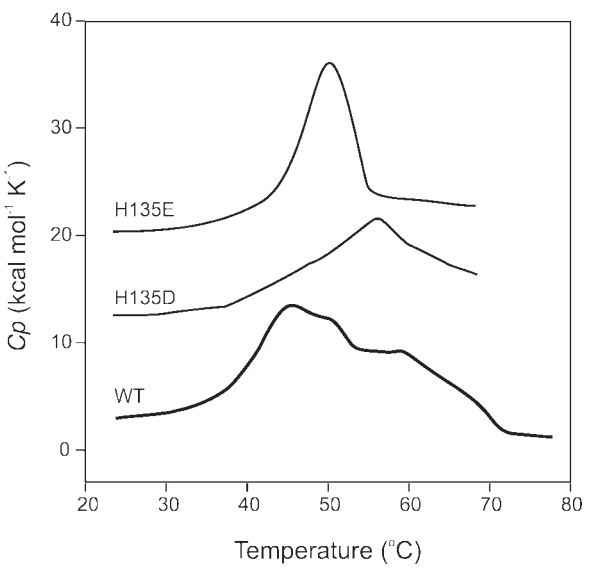

Figure 3. Thermal unfolding of the wtTAP and its variants in differential scanning calorimetry. Thermograms are normalized for protein concentration without baseline subtraction. DSC traces of H135E and H135D have been displaced along the y axis for clarity.

(Fig. 2). This binding site is well suited to octahedral Mg^{2+} coordination but responds in an unexpected way to mutations in the second sphere of the M3 metal binding site.

Wild-type ECAP binds a mixture of Mg^{2+} and Zn^{2+} in its active site.[2] An aspartate to histidine change in one ECAP residue corresponding to TAP H135 results in tetrahedral coordination of Zn^{2+} in M3, which is inhibitory to AP catalysis.[20] This mutation combined with a lysine to tryptophan change in the TAP W260 position (ECAP K328W) results in a highly active enzyme, but only at high Mg^{2+} concentrations. The ECAP D153H/K328W variant, which has similar side chain chemistry to TAP, has approximately equal activity with Co^{2+} as with Zn^{2+}, but it is most active in combinations of these metals with Mg^{2+}.[25] However, the coordination network of active sites of these variants differs from the TAP active site. ECAP 153H adjusts to directly coordinate M3, unlike in TAP, which preserves the residue 153 coordination and coordination through a water molecule. In addition, the mutated ECAP 328W does not fit into the active site but swings away, resulting in a poor model for comparison of the active site chemistry in TAP and ECAP.[26] In the current set of structures, the active site architecture is preserved to a much greater extent, making it easier to pinpoint true differences.

In TAP, the H to D change in the second coordination sphere of M3 favors Zn^{2+}, and as a consequence increases the heat stability and catalytic activity of TAP. In addition, TAP coordinates Zn^{2+} in M3 with the active but nontypical octahedral coordination, whereas the reverse change, D153H in ECAP, resulted in tetrahedral, inactive Zn^{2+} coordination. How do these two AP active sites differ?

In the wild-type TAP, the H135 backbone is stabilized by the following helix and 135(N) interaction to the preceding turn. This turn is further stabilized through side chain interactions of the small residues S131 and T134 to E151, also stabilizing R148.[9] An additional hydrogen bond between S131(O) and L133(N) forms to interact with a stretch of three glycine residues (TAP 168–170). In ECAP, this area has less backbone interaction and more side chain hydrogen bonding. The interactions are also made with longer residues in ECAP, and they continue into the region following G168-G170 in TAP, thus making thermal motions or rearrangements in this area entropically less favorable in ECAP.

The key differences in the metal selectivity between TAP and ECAP are determined by the charge transfer properties and coordination of the 135/153 side chain. The coordination sphere of the metal is critical for the function of the metal binding site,[19] because it affects both the chemistry and coordination number of the bound metal. The importance applies not only to the direct coordination but also to the second sphere of the coordination, which may provide the subtle differences to allow selection toward the preferred metal ion. Both wild-type ECAP D153 and TAP H135 are in the second coordination sphere of M3, steering the waters optimally for catalysis. However, the mutated residues behave differently in the two active sites. In the wild-type ECAP, D153 is coordinating only one water molecule and in addition is hydrogen bonded to K328, which allows charge transfer through a coordination network of waters and residues E150 and K209 (Fig. 4). When ECAP D153 is mutated to histidine, hydrogen bonding to K328 is no longer possible but instead the residue becomes suitable for direct coordination of a Zn^{2+} ion in the M3 site. The mutated ECAP 153H coordinates the metal ion directly, unlike the wt-TAP H135, which hydrogen bonds to one of the M3 waters. In ECAP, direct coordination to a side chain N-atom allows Zn^{2+} to adopt a tetrahedral coordination sphere, thus interfering with the position of the M3 waters in the catalysis.

In the mutated TAP, 135D shares its coordination between two of the M3 waters (Fig. 4). The negatively charged 135D is inserted into a neutral histidine position, which has no network for charge compensation as the ECAP site does. The mutation allows the TAP-H135D to catalyze the reaction with equal efficiency with Zn^{2+} in M3, unlike the wtTAP, which strongly prefers Mg^{2+} in combination with Zn^{2+} over Zn^{2+} alone (Table IV). This is most likely due to the fact that the mutated TAP residues still coordinate the M3 metal ion through a water network, forcing octahedral coordination of the metal ion. In addition, the H135D mutation stabilizes the enzyme toward dilution of the metal ions (Table III) and heat (Fig. 3, Table V), which might, in addition to the more charged interaction with M3, also be due to the charged and thus stronger interaction with R148.

Our results strongly support a role for the M3 in direct protonation of the leaving group phosphate or involvement in transition state stabilization.[12] The catalysis essentially requires octahedral coordination on M3, but the identity of the metal ion is of less importance. Both suggested catalytic roles benefit, from a more efficient lowering of the pK_a of the water molecule, as long as the water is correctly positioned. Zn^{2+} differs from Mg^{2+} both in its size and chemistry, providing better activation (pK_a) of the coordinated water molecules to protonate the leaving phosphate, which results in a faster k_{cat}. However, there is a price to pay for TAP catalysis from the increased activity with Zn^{2+}. The more flexible water coordination sphere of Zn^{2+} results in a greater difference in the entropic state between the bound and free enzyme active sites, thus resulting in higher K_m values in case of the Zn^{2+} binding variants. Subtle differences, such as this, are

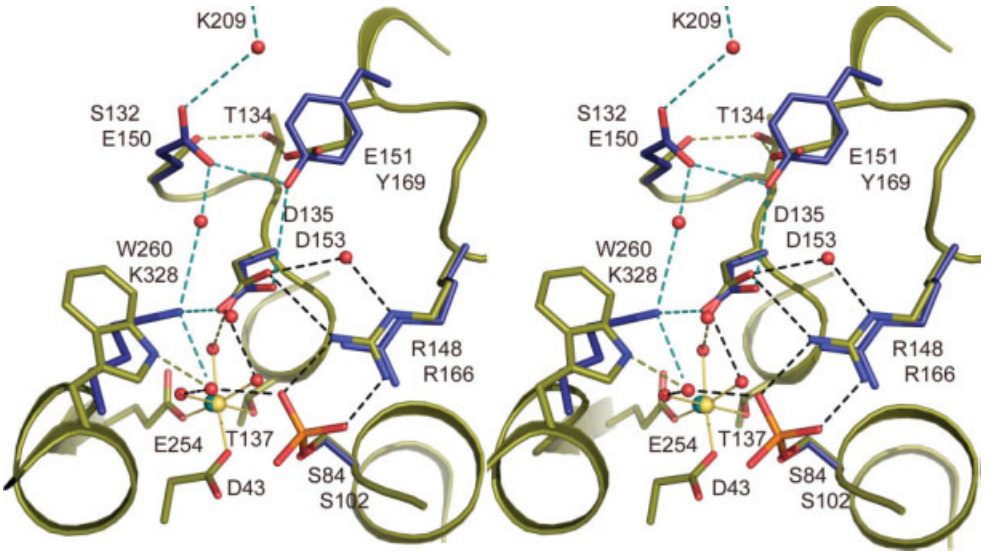

Figure 4. Superimposition of the TAP-H135D and wild-type ECAP structures in stereo. The TAP structure is shown in green, and the selected ECAP residues are shown in blue. The D135/153 residues from both structures are shown. Shared coordination in both structures is shown in black, whereas the ECAP-specific hydrogen bonds are in cyan and TAP-specific are in green.

essential to understand to support the attempts for designing more efficient APs, and in fact all applied enzymes, for the use of modern biotechnology.

Materials and Methods

Overexpression and purification of enzymes

For this study, H135D-TAP[18] was cloned into the same vector background as the wild-type and H135E-TAP.[17] Protein was expressed as before[17] but using the T7 Express LysY *E. coli* strain (New England Biolabs) and only 0.3 m*M* isopropyl thio-β-D-galactopyranoside for induction. Cells were grown, harvested, and frozen as previously.[17] One additional purification step was introduced before the gel filtration step.[17] Active fractions from the Q Sepharose fast flow (GE Healthcare) were pooled and dialyzed against 20 m*M* Tris-Cl pH 7.6, 10 m*M* $MgCl_2$ (buffer A) and loaded onto a Q Hitrap HP column (GE Healthcare). The column was washed with buffer A and eluted with a linear 0–0.2*M* gradient of NaCl in buffer A over 20 column volumes. AP eluted at ~0.1–0.14*M* NaCl. The pure proteins were stored at −20°C in 10 m*M* Tris-Cl pH 7.6, 5 m*M* $MgCl_2$, 100 m*M* NaCl, 1 m*M* DTT, and 50% glycerol. Protein concentrations for kinetic and residual activity experiments were determined with the Bradford Protein assay (Bio-Rad) with bovine serum albumin as the protein standard.

Crystallization and data collection

The H135D- and H135E-TAP variants were crystallized in hanging drops as the wtTAP[9] by mixing the protein (in 20 m*M* Tris-Cl, pH 8.0, 10 m*M* $MgCl_2$, and 0.01 m*M* $ZnCl_2$) 1:1 with 23% PEG3350, 0.2 M Na-acetate, and 0.1*M* cacodylate, pH 6.5. In addition, before crystallization, the more stable H135D-TAP was dialyzed against 10 m*M* Tris-Cl, pH 8.0 containing 1 m*M* EDTA and then against 10 m*M* Tris-Cl, pH 8.0, and 1 m*M* $ZnCl_2$, both overnight in the cold room. In addition to the standard TAP crystallization conditions, H135D-TAP crystals were grown after dialysis in the presence of 1 mM $ZnCl_2$ alone. The initial, needle-shaped H135E-TAP crystals were seeded into a 2-μl drop containing a 1:1 mixture of protein at 5 mg/ml in 20 m*M* Tris-Cl, pH 8.0, 10 m*M* $MgCl_2$, and 0.01 m*M* $ZnCl_2$ with a well solution of 23 % PEG 3350 (Fluka Ultra), 0.2 m*M* sodium acetate, and 0.1 m*M* sodium cacodylate at pH 6.5. Typically, the crystals appeared in 2–5 days, and before vitrifying, the crystals were soaked in appropriate crystallization solution containing 25% glycerol. Data were collected at ESRF beamlines ID23-1 (H135D) and ID14-2 (H135E) at 100K.

Both variants crystallized in $P2_12_12$ with approximate cell constants of $a = 70$ Å, $b = 173$ Å, and $c = 55$ Å. The images were processed in XDS[27] and analyzed with Pointless in CCP4[28] and converted to mtz format with the correct setting of the cell screw axes. Afterward, data were scaled in Scala of the CCP4 program suite, version 6.0.2.[28] A summary of the data processing and quality is presented in Table I.

Structure solution and refinement

Molecular replacement was done with Phaser[29] in the CCP4 package, version 6.0.2[28] using a monomer

of the wtTAP structure (2iuc[9]) without any ligands. The manual refinement was performed in Coot.[30] The main chain was fitted correctly from the wtTAP template, and side chains needed only small corrections. H135 residues were mutated to the correct residues from the initial maps, and the loop region (residues 315–320) was built manually starting with the highest resolution H135D-TAP structure. It was clear that the active site contained three metal ions. The identity of each was determined by comparison of the refinement rounds in Phenix[31] and inspection of the standard and anomalous (H135D-Zn^{2+}) difference electron density maps. The final round of refinement included eight TLS groups identified after model analysis at the Translation/Libration/Screw Motion Determination server[32,33] (Supporting Information Fig. 1). The groups were defined equal in both monomers. The refinement statistics are presented in Table I. The final structures are made publicly available at the protein data bank with submission codes 2w5w (H135D-3Zn^{2+}-TAP), 2w5v (H135D-2$Zn^{2+}$$Mg^{2+}$-TAP), and 2w5x (H135E-TAP) for the structures and r2w5wsf, r2w5vsf and r2w5xsf for the corresponding structure factors.

Enzymatic assay

Specific activity was determined at 25°C in 1*M* diethanolamine-Cl pH 10, 10% glycerol, 10 m*M* $MgCl_2$, and 1 m*M* $ZnCl_2$, with 5 m*M* p-nitrophenyl phosphate (Sigma). The amount of released product, p-nitrophenolate, was measured using a SpectraMax M5 96-well plate reader (Molecular Devices) at the alkaline pH absorption peak, 405 nm.

Steady-state enzyme kinetics

Steady-state enzyme kinetics were measured at 25°C, and the reaction was monitored every 10 sec. After 5 min, the reaction is complete. The program HYPER v 1.01 (John. Easterby, unpublished) was used for the determination of V_{max} and K_m values. The k_{cat} values were calculated from V_{max} using a molecular mass of 35861 Da for the enzyme. Reported values are the average of three measurements. The standard deviations do not exceed 5%.

Removal of weakly bound metals

Weakly associated metals were removed through extended dialysis. A total of 0.5 ml of 28 μ*M* protein sample was dialyzed twice in 2 l of 20 m*M* Tris-Cl, pH 7.6 for 24 hr at 4°C. After the dialysis, we added separately or in various combinations 0.1–10 m*M* $ZnCl_2$, $MgCl_2$, and $CoCl_2$ to 1.4 μ*M* protein sample. Metal–enzyme solutions were incubated at 4°C for 2 hr before activity measurements.

Thermal inactivation of enzymes

For thermal inactivation measurements, enzymes were incubated at 55 and 60°C for 120 min, samples were collected every 5 min in 20 m*M* Tris-Cl pH 7.6, 10 m*M* $MgCl_2$, 200 m*M* NaCl, and treatment stopped by incubation on ice for 30 min. The remaining activity in the samples was then measured at 25°C. Reported values are the average of at least three measurements. The standard deviations do not exceed 5%.

Differential scanning calorimetry

Measurements were performed using a MicroCal MCS-DSC instrument at a scan rate of 90 K/hr and under 2 atm pressure of nitrogen. Before the analysis, samples were dialyzed overnight against 30 m*M* 3-(*N*-morpholino) propanesulfonic acid pH 7.5, which was also used for baseline. Protein concentration for the DSC measurements was determined by the bicinchoninic acid protein assay (Pierce), and was set to ~4 mg/ml. Calorimetric enthalpies (ΔH_{cal}) were calculated from the area of the transitions, limited by a linear baseline drawn between the start and the end of the transitions and normalized for protein concentration. Datapoints more than 70°C were excluded due to the exothermic signal drift caused by aggregation.

References

1. Kim EE, Wyckoff HW (1991) Reaction mechanism of alkaline phosphatase based on crystal structures. Two-metal ion catalysis. J Mol Biol 218:449–464.
2. Stec B, Holtz KM, Kantrowitz ER (2000) A revised mechanism for the alkaline phosphatase reaction involving three metal ions. J Mol Biol 299:1303–1311.
3. Hull WE, Halford SE, Gutfreund H, Sykes BD (1976) 31P nuclear magnetic resonance study of alkaline phosphatase: the role of inorganic phosphate in limiting the enzyme turnover rate at alkaline pH. Biochemistry 15: 1547–1561.
4. Rina M, Pozidis C, Mavromatis K, Tzanodaskalaki M, Kokkinidis M, Bouriotis V (2000) Alkaline phosphatase from the Antarctic strain TAB5. Properties and psychrophilic adaptations. Eur J Biochem 267:1230–1238.
5. Le Du MH, Stigbrand T, Taussig MJ, Menez A, Stura EA (2001) Crystal structure of alkaline phosphatase from human placenta at 1.8 Å resolution. Implication for a substrate specificity. J Biol Chem 276:9158–9165.
6. Llinas P, Stura EA, Menez A, Kiss Z, Stigbrand T, Millan JL, Le Du MH (2005) Structural studies of human placental alkaline phosphatase in complex with functional ligands. J Mol Biol 350:441–451.
7. de Backer M, McSweeney S, Rasmussen HB, Riise BW, Lindley P, Hough E (2002) The 1.9 Å crystal structure of heat-labile shrimp alkaline phosphatase. J Mol Biol 318:1265–1274.
8. Helland R, Larsen RL, Asgeirsson B (2009) The 1.4 Å crystal structure of the large and cold-active *Vibrio* sp. alkaline phosphatase. Biochim Biophys Acta 1794: 297–308.
9. Wang E, Koutsioulis D, Leiros HK, Andersen OA, Bouriotis V, Hough E, Heikinheimo P (2007) Crystal structure of alkaline phosphatase from the Antarctic bacterium TAB5. J Mol Biol 366:1318–1331.
10. Oksanen E, Ahonen AK, Tuominen H, Tuominen V, Lahti R, Goldman A, Heikinheimo P (2007) A complete

structural description of the catalytic cycle of yeast pyrophosphatase. Biochemistry 46:1228–1239.
11. Le Du MH, Lamoure C, Muller BH, Bulgakov OV, Lajeunesse E, Menez A, Boulain JC (2002) Artificial evolution of an enzyme active site: structural studies of three highly active mutants of *Escherichia coli* alkaline phosphatase. J Mol Biol 316:941–953.
12. Zalatan JG, Fenn TD, Herschlag D (2008) Comparative enzymology in the alkaline phosphatase superfamily to determine the catalytic role of an active-site metal ion. J Mol Biol 384:1174–1189.
13. Wojciechowski CL, Cardia JP, Kantrowitz ER (2002) Alkaline phosphatase from the hyperthermophilic bacterium *T. maritima* requires cobalt for activity. Prot Sci 11:903–911.
14. Tibbitts TT, Murphy JE, Kantrowitz ER (1996) Kinetic and structural consequences of replacing the aspartate bridge by asparagine in the catalytic metal triad of *Escherichia coli* alkaline phosphatase. J Mol Biol 257: 700–715.
15. Murphy JE, Tibbitts TT, Kantrowitz ER (1995) Mutations at positions 153 and 328 in *Escherichia coli* alkaline phosphatase provide insight towards the structure and function of mammalian and yeast alkaline phosphatases. J Mol Biol 253:604–617.
16. Muller BH, Lamoure C, Le Du MH, Cattolico L, Lajeunesse E, Lemaitre F, Pearson A, Ducancel F, Menez A, Boulain JC (2001) Improving *Escherichia coli* alkaline phosphatase efficacy by additional mutations inside and outside the catalytic pocket. Chem biochem 2: 517–523.
17. Koutsioulis D, Wang E, Tzanodaskalaki M, Nikiforaki D, Deli A, Feller G, Heikinheimo P, Bouriotis V (2008) Directed evolution on the cold adapted properties of TAB5 alkaline phosphatase. Protein Eng Des Sel 21: 319–327.
18. Tsigos I, Mavromatis K, Tzanodaskalaki M, Pozidis C, Kokkinidis M, Bouriotis V (2001) Engineering the properties of a cold active enzyme through rational redesign of the active site. Eur J Biochem 268: 5074–5080.
19. Lee YM, Lim C (2008) Physical basis of structural and catalytic Zn-binding sites in proteins. J Mol Biol 379: 545–553.
20. Murphy JE, Xu X, Kantrowitz ER (1993) Conversion of a magnesium binding site into a zinc binding site by a single amino acid substitution in *Escherichia coli* alkaline phosphatase. J Biol Chem 268:21497–21500.
21. D'Amico S, Marx JC, Gerday C, Feller G (2003) Activity-stability relationships in extremophilic enzymes. J Biol Chem 278:7891–7896.
22. Heikinheimo P, Lehtonen J, Baykov A, Lahti R, Cooperman BS, Goldman A (1996) The structural basis for pyrophosphatase catalysis. Structure 4:1491–1508.
23. Heikinheimo P, Tuominen V, Ahonen A-K, Teplyakov A, Cooperman BS, Baykov A, Lahti R, Goldman A (2001) Towards a quantum-mechanical description of metal assisted phosphoryl transfer in pyrophosphatase. PNAS 98:3121–3126.
24. Dokmanic I, Sikic M, Tomic S (2008) Metals in proteins: correlation between the metal-ion type, coordination number and the amino-acid residues involved in the coordination. Acta Cryst D 64:257–263.
25. Wojciechowski CL, Kantrowitz ER (2002) Altering of the metal specificity of *Escherichia coli* alkaline phosphatase. J Biol Chem 277:50476–50481.
26. Wang J, Stieglitz KA, Kantrowitz ER (2005) Metal specificity is correlated with two crucial active site residues in *Escherichia coli* alkaline phosphatase. Biochemistry 44:8378–8386.
27. Kabsch W (1993) Automatic processing of rotation diffraction data from crystals of initially unknown symmetry and cell constants. J Appl Cryst 26:795–800.
28. Collaborative Computational Project N (1994) The CCP4 suite: programs for protein crystallography. Acta Cryst D 50:760–763.
29. McCoy AJ, Grosse-Kunstleve RW, Storoni LC, Read RJ (2005) Likelihood-enhanced fast translation functions. Acta Cryst D 61:458–464.
30. Emsley P, Cowtan K (2004) Coot: model-building tools for molecular graphics. Acta Cryst D 60:2126–2132.
31. Adams PD, Grosse-Kunstleve RW, Hung LW, Ioerger TR, McCoy AJ, Moriarty NW, Read RJ, Sacchettini JC, Sauter NK, Terwilliger TC (2002) PHENIX: building new software for automated crystallographic structure determination. Acta Cryst D 58:1948–1954.
32. Painter J, Merritt EA (2006) Optimal description of a protein structure in terms of multiple groups undergoing TLS motion. Acta Cryst D 62:439–450.
33. Painter J, Merritt EA (2006) TLSMD web server for the generation of multi-group TLS models. J Appl Cryst 39:109–111.